



# Two stage self-adaptive cognitive neural network for mixed noise removal from medical images

Vishal H Shah<sup>1</sup> · Prajna Parimita Dash<sup>1</sup>

Received: 15 October 2021 / Revised: 12 January 2023 / Accepted: 18 April 2023 /  
Published online: 10 June 2023

© The Author(s), under exclusive licence to Springer Science+Business Media, LLC, part of Springer Nature 2023

## Abstract

In the current era of technological advancements where convergence of social mobility analytics and clouds enabled the end users in capturing precise medical images on the go but also had lead incorporation of unusual noises too. One such scenario is the combination of both Additive White Gaussian Noise (AWGN) along with impulse noise that are added during acquisition and post-processing of medical images which hampers the overall medical image processing where identification of region of interest is pretty important. The noises not only affect the textures but also could plays at the pixelate level. In this work, a patch transformation technique for mixed noise removal and the bilateral filtering approach for edge preservation have been associated with the cognitive neural network model to remove the noise from medical images. The self adaptation of the network identifies the presence of mixed noise and generate the training dataset with the noisy patches along with the denoised patches. The proposed two stage self adaptive cognitive neural network model (SACNN) successfully retains the edge information along with denoising of the images. The performance of SACNN model is compared with other state-of-the-art techniques through various performance matrices. Statistical analysis such as, Signed test, Wilcoxon Signed rank test and Friedman test are also carried out to investigate the dominance of proposed approach over others.

**Keywords** Mixed noise · Convolutional Neural Network (CNN) · Cognitive neural network · Medical image denoising · Statistical analysis

---

Prajna Parimita Dash has contributed equally to this work

✉ Vishal H Shah  
vishalhshah@bitmesra.ac.in

Prajna Parimita Dash  
ppdash@bitmesra.ac.in

<sup>1</sup> Department of Electronics and Communication Engineering, Birla Institute of Technology, Mesra, Ranchi, 835215, Jharkhand, India

# 1 Introduction

Advancements in low-cost imaging and computational devices have made non-invasive medical imaging a most adopted platform for detection of various abnormalities in different organs of body. The growth of sensing technologies has revolutionized the medical science in the most unprecedented manner. The importance of medical imaging in the clinical procedures is well known. With these advancements, detailed hyper local level information could be obtained which would be utilized in making significant progress in prognosis as well as diagnosis. These developments would also help the medical practitioners in image enhancements to augment regions of interest to image segmentation and object recognition. Medical practitioners diagnose and examine various diseases from different medical modalities, such as, X-Ray, Computed Tomography (CT), Magnetic Resonance Imaging (MRI), Ultrasound, Positron Emission Tomography (PET), and Single Photon Emission Computed Tomography (SPECT) etc. The importance of this also makes it more susceptible to be corrupted. The corruptions of these medical images are caused by various noises due to disturbances in the acquisition and post processing of the captured images. Presence of noises produces unwanted artifacts on the acquired images. These noises not only affect the region of interest but also affects the pixelate distribution thereby causing the loss of textures, edges and many of the important features. This ultimately hampers with the exact diagnosis and prognosis of the diseases. Therefore, the medical images must be noise free and the edges need to be sharp for its suitability in precise and accurate diagnosis [10]. The method of image acquisition and presence of various other disturbances are two major contributors of introduction of various spurious noises, such as, Gaussian, impulse, speckle etc. [9]. These noises significantly degrade the quality by reducing the amount of information in the image. An in-depth review has been conducted on various filtering algorithms to de-noise images in [6].

Various classical filters like Gaussian [4], Mean [7], Median [13], non-local mean [3] are designed for suppressing various spurious noises. However, all these filters are usually fixed filters, and work effectively only for a particular type of noise. To overcome this bottleneck, different variants of Artificial Neural Network (ANN) based adaptive filter models have been implemented by researchers [1]. It has been found that noise removal as well as edge preservation to maintain the region of interest varies from one case to other and hence adaptability is the key. This is where ANNs could be a game changer which will do wonders once the hyper local information is fed to them.

Some of the most widely used ANNs are feed forward neural network, convolution neural network, pulse coded neural network and wavelet neural network etc. [16]. Although lots of techniques are available for the suppression of noise, vary few approaches have been suggested for suppressing mixed noises from the images [24]. The existing techniques for mixed noise suppression firstly detect the type of noise, and thereby invokes specific filter needed to remove the noise [31]. Moreover, the performance of most of the available approaches for suppressing mixed noise cannot effectively restore the edges of the images [12, 19, 37]. During the mixed noise removal, the texture information gets affected, thereby, loosing some edge information, which is a major parameter in the process of medical image diagnosis. Thus, edge preservation is an essential requirement in medical image processing. This motivates to embed the edge preservation stage along with the mixed noise removal. Conductive to this issue, in this paper, a two stage self-adaptive cognitive neural network (SACNN) for mixed noise removal from medical images has been proposed.

In the proposed technique, the noise removal is achieved for any type of noise by detecting the pixel to be replaced in the corrupted image. The proposed SACNN is trained for the replacement of noisy pixel from corrupted image. Thus, the proposed approach not only enables reduction in the loss in the quality of the images through mixed noise suppression but also enables edge preservation at the global level to facilitate the preservation of edges as well as pixel level features for efficient decision making.

To achieve these two objectives of mixed noise suppression and edge preservation simultaneously, in this research article, a novel two-stage cognitive learning assisted algorithm has been proposed. In the first stage, mixed noise is removed with a Self-Adaptive Cognitive Neural Network (SACNN) based pixel replacement technique. Further in the second stage, adaptive bilateral filtering guided by cognitive neural network is used to sharpen the pixels present in the edges. The parameters for adaptive bilateral filtering are obtained by SACNN by exploiting the global and local characteristics of the image. The important contribution of this study is outlined as below:

1. A two stage Self-Adaptive Cognitive Neural Network (SACNN) model has been proposed by combining the mixed noise removal stage and edge preservation stage, which effectively suppresses the mixed noise from the medical images, retaining the edge information.
2. A patch transformation approach, by considering difference of variance of the pixels with their neighbourhood is adopted to find the noise-free patches. Edge preservation of the patches is done by using the bilateral filtering techniques. For the training of the SACNN model, a training data set is generated using the edge features of the noisy patches as well as noise-free patches.
3. Different Hinge loss functions are fed to the network for the loop control of the model. The model gives the output based on best performance of one of them.
4. The MRI, CT and Ultrasound datasets have been collected from the standard repository at [<https://www.kaggle.com/>] in JPEG format for implementation of our proposed approach. Furthermore, some real time data have been collected from Om Hospital, Raipur (C.G) for the validation of the proposed method.

The remaining part of the paper has been laid down as follows: Section 2 of the paper describes the related work in the field of medical image denoising by using variants of ANN and deep learning techniques. Section 3 presents the methodology for design of proposed model for mixed noise removal filter and edge preservation. Section 4 deals with the experimental results and discussion supported by both quantitative and qualitative analysis. The work has been concluded in section 5.

## 2 Related work

This section represents the work of various researchers in the recent decade, related to the proposed technique. Lin et al. [20] proposed a switching bilateral filter for universal noise removal. They proposed noise removal in two-stages, detection followed by filtering operation. Sorter Quadrant Median Vector (SQMV) detected the pixel, which are categorized as impulse noise and Gaussian noise. A range filter is implemented along with the bilateral filter to switch between Gaussian and impulse mode. Their proposed algorithm basically assumed that there are few pixels which are neither effected by Gaussian noise nor by impulse noise, which is however not always the possibility in case of mixed noise removal

technique. Li et al. [19] proposed a mixed noise filter to remove mixture of Gaussian and random impulse noise simultaneously. The basic idea of trilateral filter and similarity principle is combined to create a new filter. Here, tuning of control parameter of trilateral filter is realized using two empirical formulas. But the approach worked only when the impulse noise distribution is uniform across the image. Xiong et al. [38] proposed a universal noise filter based on non-local means. The approach has two-stages of detection and filtering that work one after another. Pixels are divided into four categories based on new metric called Robust Outlyingness Ratio (ROR) which measures the impulsiveness in the pixel. Non-local means (NL) based filtering is implemented with parameter optimized for each cluster. Hongjin et al. [23] integrated Adaptive Directional Weighted Mean Filter (ADWMF) and Improved Adaptive Anisotropic Diffusion (IAAD) model to remove mixed noises from the image. Impulse noise is removed using ADWMF and Gaussian noise is removed using IAAD model. However, the method cannot remove salt and pepper noise and the restoration effectiveness is also reduced in case of higher noise density. Thus, one of the prominent limitations of the previous studies is highlighted as loss in the quality of the images due to mixed noises.

Turkmen et al. [35] used ANN to detect whether pixel is corrupted with random impulse noise or not. Once the corrupted pixels are detected, edge preserving regularization is done to restore the pixel. However, the detection of corruption of the pixel is based only on local neighborhood without considering the global characteristics of the image, and hence image cannot be denoised completely. Thus, second limitation is that only local features were preserved and not the global ones. Guo et al. separately restored the low and the high frequency of image components based upon nonlocal self-similarity learning (NSS) [11]. Nair et al. [26] proposed a predictive adaptive switching median filter to filter out impulse noise from images. In their work, the Feed Forward Neural Network (FFNN) is used to detect impulse noise. The detected impulse noise is filtered out using a modified median filter. The corrupted pixels in a  $3 \times 3$  sliding window are detected using feed forward neural network. The computation overhead increases linearly with the increase in intensity of noise due to the requirement of more iteration for denoising. Recently, several researchers have proposed different optimization technique based adaptive filters for noise elimination from medical images and have successfully denoised the images [14, 15, 18]. However, such techniques largely rely upon the population sizes for accuracy and speed.

Li et al. [17] have applied iterative technique to reduce the complexity involve in splitting minimization problems. Liu et al. [22] presented an overview of deep learning based de-noising models. Here denoising models based on Convolutional Neural Network (CNN), Pulse Coded Neural Network (PCNN) and Wavelet Neural Network (WNN) were briefed. Third limitations or say a major bottleneck in these denoising models is that there is no fixed standard or basis for setting the parameters of the model. Radlak et al. [28] applied deep learning for impulse noise removal from the images. Deep learning convolutional based neural network detects the pixels corrupted by impulse noise in the image. These pixels are then restored back using an adaptive arithmetic mean filter. Impulse detection and restoration are realized in two different stages resulting in longer time for restoration. The detection of impulse noise in each category is decided using deviation-based decision rules and there is no automated way to choose the decision rules. Zhang et al. [43] integrated a set of convolutional neural network denoisers to remove the Gaussian noise. Due to involvement of number of discriminative denoisers and a greater number of iterations, the time requirement for denoising is very high. To address these difficulties, Zhang et al. [42] proposed a Feed Forward Convolutional Neural Network (FFCNN) for image denoising. The method

is found to be suitable for Gaussian noise denoising having different noise levels. Here, single CNN model can address multiple tasks of Gaussian denoising, single image super resolution and JPEG image de-blocking simultaneously. The computation overhead is very high, and it needs special purpose graphical processing units for denoising. The authors in [25, 33] utilized adaptive bilateral filter (ABF) for removal of the noises in MR images. They used binary thresholding and Fuzzy Recurrent Neural Network (FR-Net) as segmentation techniques for effective and efficient detection of the tumor regions. Turkmen et al. [34] have used Artificial Neural Network (ANN) to denoise the image corrupted by random valued impulse noises. The gradient values deviation of pixels by random impulse noises is detected using the ANN. In this method the median filtering is used to restore the pixels detected by ANN. The training and testing time for the implementation of this approach is very high. Liu et al. [21] integrated deep learning with non-local mean filtering algorithm to remove noises from the image. Deep learning provides the best parameter setting for non-local mean filtering algorithm to achieve a better denoising. Though their method can achieve higher PSNR, enough smoothing is not achieved, and training set is also very limited. Hence to overcome the above-mentioned limitations and difficulties for achieving good denoised image with all the edge information preserved, the current work proposes two stage Self-Adaptive Cognitive Neural Network (SACNN) approach to remove mixed noise from medical images along with edge preservation.

### 3 Proposed approach: Two stage Self-Adaptive Cognitive Neural Network (SACNN) for mixed noise removal from medical images

Neural networks are found to be very effective in spatial cognition because of their inherent capability for adapting to the fed inputs and has been effectively used in solving complex problems on visual pattern recognition. Cognitive learning plays an important role in the estimation and detection of noisy pixels in an image. A two-stage SACNN model for mixed noise removal has been proposed in this research article.

The two-stages in the proposed approach are mixed noise removal and edge preservation in sequence. Each of the above two-stages is guided by Learning Assisted Cognitive Neural Network (LACNN) [32]. The overall flow of the proposed work is delineated in the following Fig. 1. The medical images are processed for the mixed noise removal and subsequently edge preservation. The processed images are further evaluated based on the performance evaluation matrices.

#### 3.1 Mixed noise removal

The pixels of the gray scale image  $N_{i,j}$  affected with mixed noise is represented as

$$N_{i,j} = \begin{cases} O_{i,j} + a_{i,j} & \text{for probability of } p \\ IN_{i,j} & \text{for probability of } 1 - p \end{cases} \quad (1)$$

where,  $O_{i,j}$  is the original pixel value,  $a_{i,j}$  is the Gaussian noise value and  $IN_{i,j}$  is the impulse noise. The Gaussian noise and impulse noise affects the pixel with a probability of  $p$  and  $1 - p$ . While existing solutions firstly classify the noisy medical images and then apply noise specific denoising approach, the proposed work integrates the classification and filtering in a single step using cognitive neural network. The distribution of mixed noise cannot be described by a specific function, and hence, any one filter cannot successfully

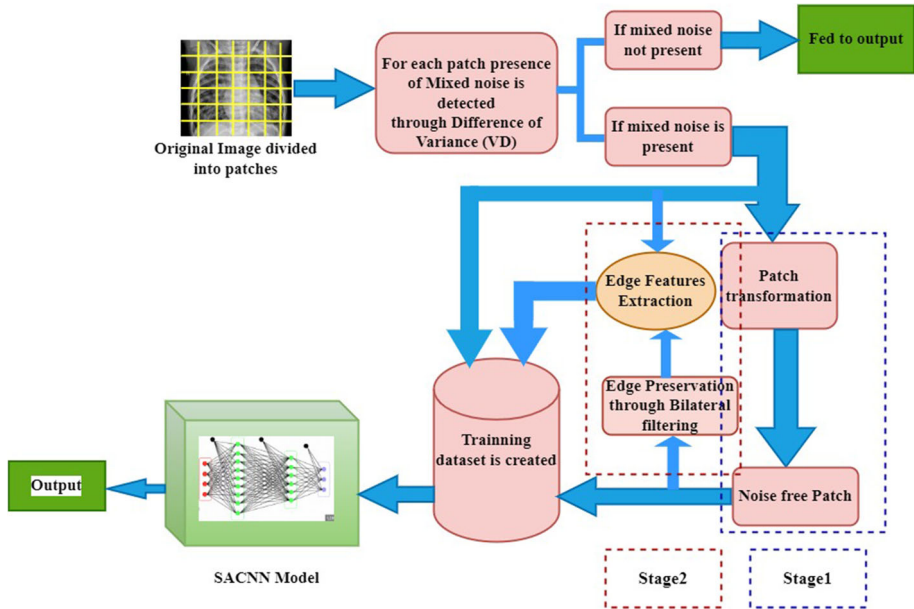


Fig. 1 Work flow of the proposed work

suppress the mixed noise in an image. Hence, this noise is normally handled by considering  $m \times m$  local window or patches. Deep convolutional model as proposed by [27] to replace the noisy patch with a noiseless patch involves many layers of convolutions and thereby take longer time for training as well as transformation. The proposed SACNN model uses a three layer feed forward neural network as shown in Fig. 2.

The training set for the neural network is prepared by splitting the noisy image into  $m \times m$  patches. The proposed training model is shown in Fig. 3. Each of the patches is first investigated for the presence of mixed noise based on the variance of gray level differences. To achieve this the steps in sequence are as follows:

1. The gray level variance of all pixels in a patch is

$$AV_{i,j} = \frac{\sum_{k=1}^{m^2} (g_{s_k r_k} - M_1)^2}{m^2} \tag{2}$$

where,  $g_{s_k r_k}$  is the gray level value of the pixel  $p_{s_k r_k}$  and  $M_1$  is the mean gray level of all pixels in the local window

2. Gray level variance of neighborhood pixels of center pixel is calculated as

$$NV_{i,j} = \frac{\sum_{k=1}^{m^2-1} (g_{s_k r_k} - M_2)^2}{m^2 - 1} \tag{3}$$

$M_2$  is the mean gray level of neighborhood pixel of center pixel.

3. The difference of variance is

$$VD = abs(AV_{i,j} - NV_{i,j}) \tag{4}$$

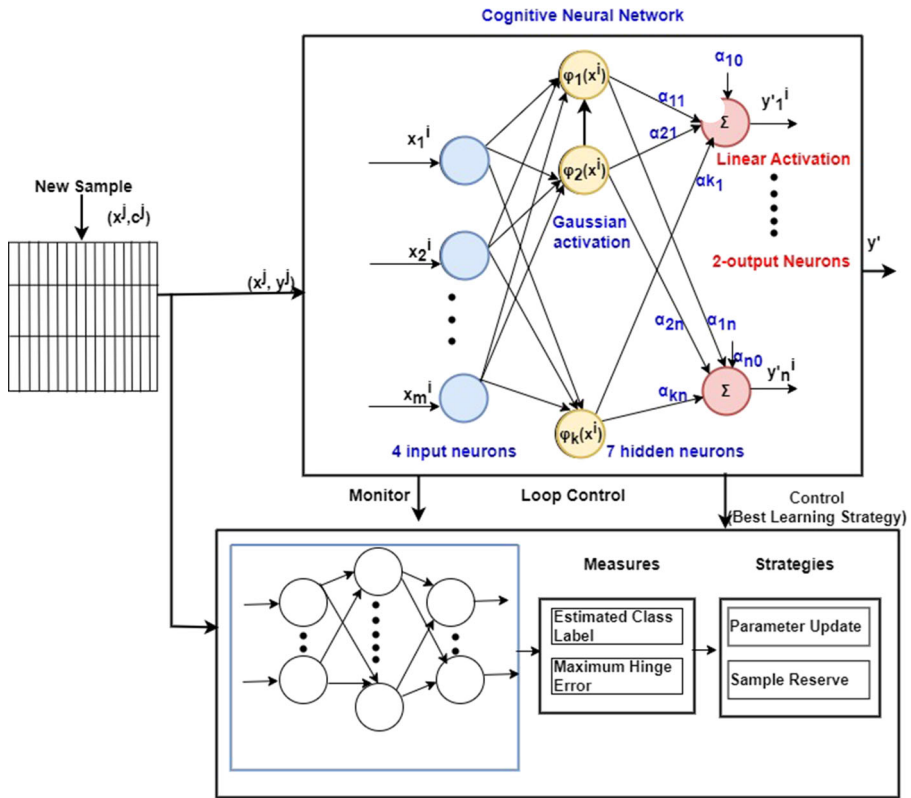


**Fig. 2** Self Adaptive Cognitive Neural Network (SACNN) Model

4. If the variance  $VD$  is greater than a threshold  $T$ , then the patch is decided to have mixed noise, and is used for the next stage of construction of output noise free patch.

The pseudo code of the algorithm for detection of mixed noise patch in our proposed SACNN has been described in Algorithm 1:

For each of the input patches where mixed noise is detected are considered for noise elimination. The output noise free patch ( $I_T$ ) is constructed as follows:

1. Centering the  $m \times m$  patch at  $(i,j)$ , four directional templates are designed as shown in Fig. 3.
2. The sum of absolute gray level difference between the center and neighborhood pixel is computed on each of the four directions.
3. The direction with minimum sum of absolute gray level difference is selected.
4. Gray level of the center pixel is replaced by weighted mean gray level of the pixel along the selected direction.
5. The gray level of the center pixel is further transformed by applying Wiener filter as below

$$W(g_{i,j}) = z + \frac{v^2 - \sigma^2}{v^2} (g_{i,j} - z) \tag{5}$$

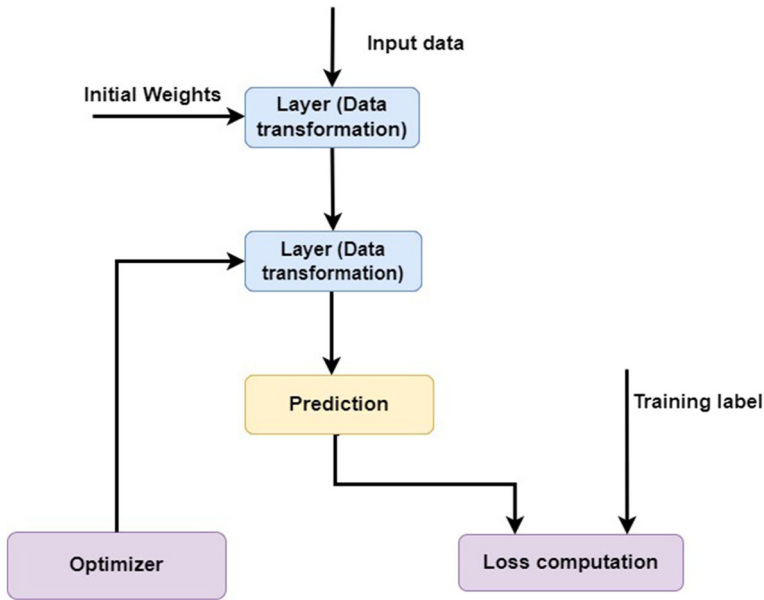


Fig. 3 Training model for neural network

**Require:** window, threshold  $T$

**Ensure:** True or false

- 1:  $M \leftarrow 0$ ;
- 2: all pixels in the window
- 3:  $M = M + \text{gray level variance of pixel as in Eq 2}$
- 4: end
- 5:  $M = M / \text{total number of pixels in window}$
- 6:  $CM = \text{Calculate gray level variance of center pixel as in Eq 3}$
- 7: **if**  $abs(M - CM) > T$  **then**
- 8:     Return True
- 9: **else**
- 10:     Return False
- 11: **end if**

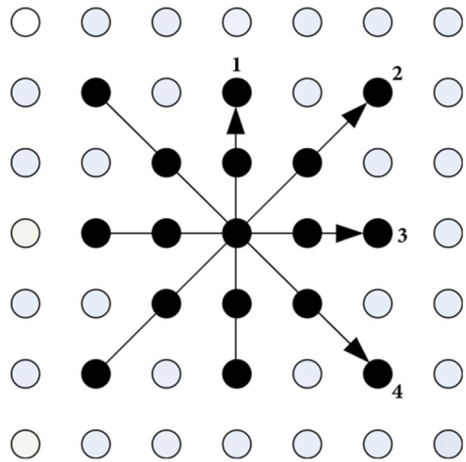
**Algorithm 1** Detect Mixed Noise.

where,  $g_{i,j}$  is the pixel value of the center pixel after step 4,  $z$  is the mean value of gray level of pixels in  $m \times m$  patch,  $v$  denotes the standard deviation of gray level of pixels in the  $m \times m$  patch,  $\sigma$  is the standard deviation of the Gaussian noise.

The pseudo-code of the algorithm for the patch transformation in the proposed SACNN filter is as briefed in Algorithm. 2.



**Fig. 4** Directional templates (Pixel Matrix)



**Require:**  $m \times m$  patch

**Ensure:** transformed patch

- 2: **For**  $i$ = four directions in Fig. 4  
Sum of gray difference[ $i$ ] = calculate in direction  $i$  using Eq 2
- 4:  
Minimum direction = Minimum index (Sum of gray difference [ $i$ ])
- 6: Center pixel = mean (gray difference in minimum direction)  
transformed=Apply Weiner filter on patch using Eq 5.
- 8: Return transformed

**Algorithm 2** Transform (Fig. 4).

Hence, each of the corresponding output patch for the input patch is

$$O = \begin{cases} I & \text{if } I \text{ is not detected as mixed noisy} \\ I_T & \text{if } I \text{ is detected as mixed noisy} \end{cases} \quad (6)$$

With the input patch  $I$  as input and  $O$  as output, the training dataset is constructed. The proposed Self-Adaptive Cognitive Neural Network (SACNN) filter is trained with the training dataset with the parameters shown in Table 1.

**Table 1** Parameters of Cognitive Neural Network

Number of layers	3
Input neurons	$m \times m$
Hidden layer neurons	$2 \times m \times m - 1$
Output neurons	$m \times m$
Hidden layer function	Gaussian activation
Output layer function	Linear activation

**Table 2** Hinge loss functions

Classifier	Objective function: Hinge Loss Function
Linear Classifier [5]	$\max\left(0, 1 + \frac{\max_{y \neq t} w_{y,x} - w_{t,x}}{\gamma}\right)$
Linear Classifier [36]	$\sum_{y \neq t} \max\left(0, 1 + \frac{\max_{y \neq t} w_{y,x} - w_{t,x}}{\gamma}\right)$
Quadratically smoothed convex function [41]	$\begin{cases} \frac{1}{2\gamma} \max(0, 1 - t_y^2) & \text{for all } t_y \geq 1 - \gamma \\ 1 - \frac{\gamma}{2} - t_y & \text{Otherwise} \end{cases}$

The output of the neural network with k hidden layer is given as

$$y_j^i = \alpha_{j0} + \sum_{k=1}^K \alpha_{jk} \phi_k(X^i), \quad j = 1, 2, 3...n \tag{7}$$

where,  $N$  is the number of output layer neurons,  $\alpha_{j0}$  is basis to the  $j$  output neuron,  $\alpha_{jk}$  is the weight connecting  $j$  to  $k^{th}$  neuron,  $\phi_k(X^i)$  is the response of  $k^{th}$  hidden neuron to input  $X^i$  modeled as  $\phi_k(X^i) = \exp\left(-\frac{\|x^i - \mu_k\|^2}{\sigma_k^2}\right)$ . Here  $\mu_k$  and  $\sigma_k$  represent the center and width of  $k^{th}$  hidden neuron respectively.

The loop control approach is implemented to make the model self-adaptive using hinge loss function as cost function [29]. Different hinge loss functions that have been used by previous researchers are shown in Table 2. Here  $t$  is the class label or target label,  $w_t$  and  $w_y$  are the model parameters.

The training is repeated iteratively till the hinge error is minimized. Here all these hinge loss functions are considered, and one that provide better accuracy is considered for predicting noise free patch for the noisy patch.

### 3.2 Edge preservation

Bilateral Filtering (BF) has the property of preserving edges in the image [40]. BF applies a weighted sum of the pixels in local neighborhood to preserve the edges. The output of BF on a pixel at position  $x$  is given as

$$BF(x) = \frac{\sum_{y \in N(x)} e^{-\frac{\|y-x\|^2}{2\sigma_d^2}} e^{-\frac{\|t(y)-t(x)\|^2}{2\sigma_r^2}} t(y)}{\sum_{y \in N(x)} e^{-\frac{\|y-x\|^2}{2\sigma_d^2}} e^{-\frac{\|t(y)-t(x)\|^2}{2\sigma_r^2}}} \tag{8}$$

where,  $t(x)$  is the noisy pixel value at  $x$ ,  $N(x)$  is the neighborhood of  $x$ ,  $\sigma_d$  and  $\sigma_r$  are the filter parameters that limit the value of pixel in the specified intensity range. The proposed work has worked out the limitation of local neighborhood by taking the Region of Interest from the global perspective through their augmentation. In Adaptive Bilateral Filters (ABF) [39], the filter parameters are adjusted based on local and global characteristics of the image. The ABF is having two different values of filter parameters for each pixel by considering  $\sigma_d$  and  $\sigma_r$ .

$$\sigma_d = \sigma_d(x, y) \tag{9}$$

$$\sigma_r = \sigma_r(x, y) \tag{10}$$

The decision of filter parameters depends on the edge characteristics of image such as, entropy of patch ( $E_p$ ), entropy of gradient of patch ( $E_{gp}$ ) and two eigen values of structure tensor for patch ( $L_1, L_2$ ).

Entropy of patch is calculated for all pixel values in the patch using Shannon entropy [30]. It is calculated as:

$$E_p = - \sum_{h=0}^B p(h) \log_2(p(h)) \tag{11}$$

where,  $p(h)$  is the probability of pixel  $h$  in  $p$ . The entropy is 0 when all pixel values are same and is maximal when  $p(h)$  has uniform distribution. The losses incurred due to mixed noises thus, would be compensated using the information centric entropy value.

Entropy of gradient of patch ( $E_{gp}$ ) is found out by considering the gradient for all pixels in the patch, and by calculating the Shannon entropy. Gradient is calculated in vertical and horizontal directions as

$$g(x, y) = \sqrt{[i_x(x, y)]^2 + [i_y(x, y)]^2} \tag{12}$$

$i_x(x, y)$  is the gradient along the  $x$  direction calculated as

$$i_x(x, y) = i(x, y) - i(x - 1, y) \tag{13}$$

Similarly,  $i_y(x, y)$  is the gradient along the  $y$  direction that can be calculated as

$$i_y(x, y) = i(x, y) - i(x, y - 1) \tag{14}$$

The structure tensor [2] represents the gradient or edge information. Structure tensor is represented in matrix form as

$$S = \begin{bmatrix} i_x^2 & i_x i_y \\ i_x i_y & i_y^2 \end{bmatrix} = \begin{bmatrix} J_{11} & J_{12} \\ J_{21} & J_{22} \end{bmatrix} \tag{15}$$

Eigen transformation is applied to the  $S$  matrix to get the Eigen values ( $L_1, L_2$ ) as (16) and (17).

$$L_1 = \frac{1}{2}(J_{11} + J_{22} + \sqrt{(J_{11} - J_{22})^2 + 4J_{12}^2}) \tag{16}$$

$$L_2 = \frac{1}{2}(J_{11} + J_{22} - \sqrt{(J_{11} - J_{22})^2 + 4J_{12}^2}) \tag{17}$$

A dataset of image patches with the edges information in it are processed with various values of  $\sigma_d, \sigma_r$ .  $E$  is considered to be the cost function which is mathematically expressed as:

$$E = - \sum_{j=0}^{M-1} PSNR(BF(t), t) \tag{18}$$

where,  $t$  is the image patch and  $BF(t)$  is the de-noised image after bilateral filtering. The value of  $\sigma_d, \sigma_r$  at which the  $E$  is minimum are selected. Once the optimum value is found, four features i.e.,  $E_p, E_{gp}, L_1,$  and  $L_2$  are extracted. A training dataset with these features as input and  $\sigma_d, \sigma_r$  as the output is constructed.

The proposed SACNN is trained with the training dataset. The parameters of the cognitive network are depicted in Table 3:

**Table 3** Parameters of SACNN for edge smoothing

Number of layers	3
Input neurons	4
Hidden layer neurons	7
Output neurons	2
Hidden layer function	Gaussian activation
Output layer function	Linear activation

## 4 Experimental results and discussion

The simulation task is performed in a *MATLAB<sup>R</sup>* programming environment on a personal computer having specification of Intel Core *i7 @ 1.80 GHz*, 8 GB of RAM, 64-bit bus and Windows 10 Operating system. All the Medical images, viz. MRI, US, X-Ray and CT scan, were collected from a benchmark dataset [<https://www.kaggle.com/>] in JPEG format. The images are mixed with different level of AWGN plus random impulse noises to create noisy images. The standard deviation  $\sigma$  of AWGN is varied from 5 to 15 in step length of 5. The random impulse noise is varied from 10% to 60% in step length of 10%. The performance of the proposed algorithm is compared with some state-of-the-art mixed noise removal methods such as, (ADWMF + IAADM Model) proposed in Hongjin et al. [23], Tri-lateral Filter (TF) proposed by Garnett et al. [8], Switching Bilateral Filter (SBF) proposed by Lin et al. [20], Mixed Noise Filter (MNF) proposed by Li et al. [19]. The performance of the proposed technique is evaluated through subjective as well as objective evaluation. Furthermore, the statistical testing is also carried out for validation of the statistical stability of the proposed technique.

### 4.1 Subjective evaluation:

Some of the results of the proposed SACNN based method are delineated in Figs. 5, 6 and 7. In Fig. 5 results of three different MRI images (Image1, Image2 and image3) are shown. The first column represents the original images, the second column represents the noisy images (with added gaussian and impulse noise) with a PSNR value of 22.11db . The third column depicts the intermediate results obtained without edge preservation stage. The final output using both mixed noise removal as well as the edge preservation stages, are shown in the fourth column. From the output images, it is observed that for most of the cases the quality has been improved. The quality of the results are also validated through a medical expert (Doctor, from OM Hospital, Raipur).

### 4.2 Objective evaluation

The qualitative evaluation of the proposed technique has been conducted through evaluating four performance indices, i.e., average values of Peak Signal Noise Ratio (PSNR), Feature Similarity Index Measure (FSIM), Mean Absolute Error (MAE), and Structural Similarity Index Measure (SSIM). The proposed technique has been validated experimentally with total 100 images. The results for average PSNR and average FSIM for different values of  $\sigma$ , i.e.,  $\sigma = 5, 10$  and 15 at  $p = 50\%$  and at  $p = 60\%$  in order to have a fair comparison have been considered and represented in Table 4.

The average PSNR value of filtered image obtained from the proposed SACNN method applied on MRI image is 9.76% higher compared to MNF method, 10.91% higher compared

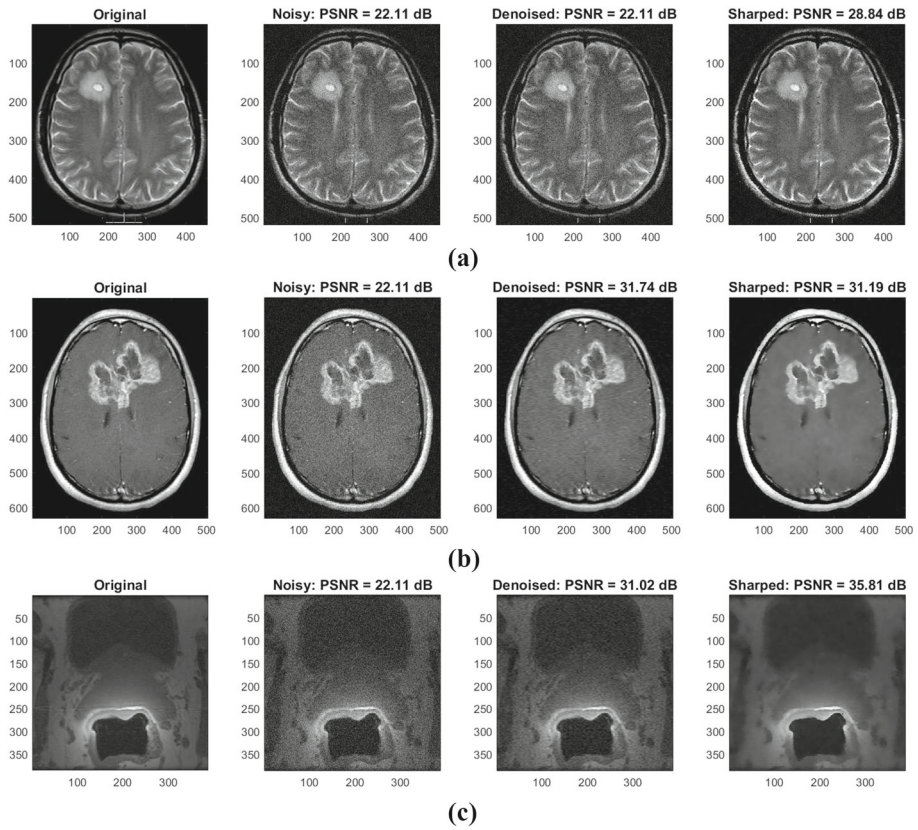


Fig. 5 Filtered MRI Images by proposed SACNN Model: (a) Image1 (b) Image2 (c)Image3

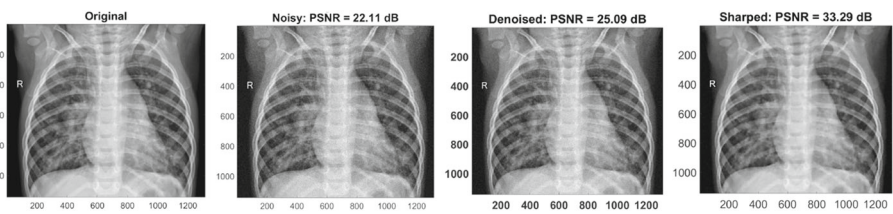


Fig. 6 Filtered X-Ray images by the proposed SACNN Model

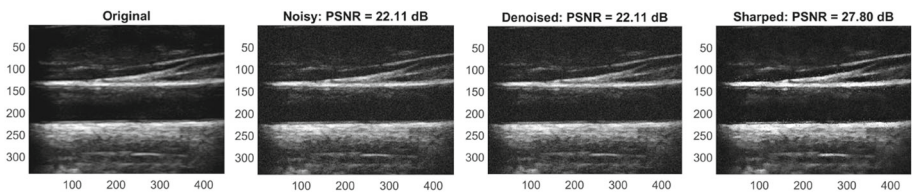
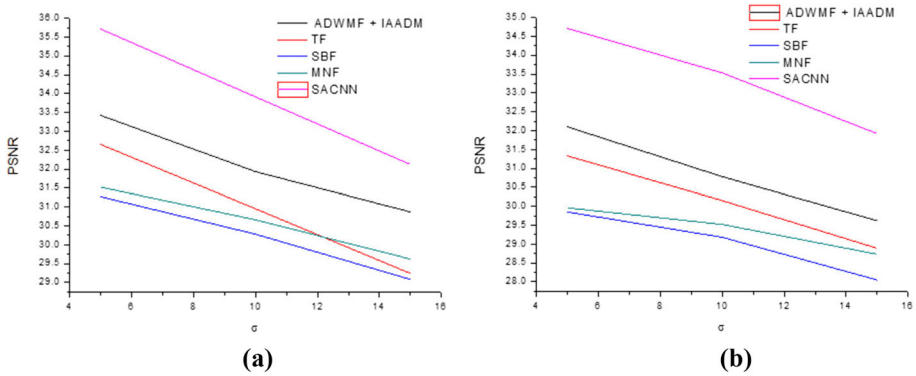


Fig. 7 Filtered Ultrasound images by proposed SACNN Model

**Table 4** Average PSNR and Average FSIM at  $p = 50\%$  and  $p = 60\%$

$\sigma$	Avg. PSNR						Avg. FSIM					
	ADWMF	TF	SBF	MNF	SACNN	IAADM	ADWMF	TF	SBF	MNF	SACNN	IAADM
	+						+					
	IAADM						IAADM					
<b>p = 50 %</b>	5	33.42	32.65	31.27	31.52	<b>35.71</b>	0.9799	0.9711	0.9676	0.9690	<b>0.9892</b>	
	10	31.93	30.95	30.28	30.66	<b>33.91</b>	0.9650	0.9548	0.9566	0.9576	<b>0.9765</b>	
	15	30.87	29.24	29.08	29.62	<b>32.12</b>	0.9497	0.9254	0.9396	0.9421	<b>0.9623</b>	
<b>p = 60%</b>	5	32.10	31.33	29.85	29.96	<b>34.71</b>	0.9686	0.9650	0.9606	0.9604	<b>0.9782</b>	
	10	30.78	30.15	29.18	29.52	<b>33.53</b>	0.9538	0.9483	0.9440	0.9453	<b>0.9635</b>	
	15	29.62	28.89	28.05	28.73	<b>31.92</b>	0.9341	0.9252	0.9241	0.9274	<b>0.9414</b>	



**Fig. 8** (a) Comparison of PSNR at  $p = 50\%$  (b) Comparison of PSNR at  $p = 60\%$

to SBF method, 8.76% higher compared to TF method and 5.42% higher compared to ADWMF + IAADM model at  $p = 50\%$ . The results for PSNR values obtained from all the approaches for different values of  $\sigma$  at  $p = 60\%$  is also tabulated in Table 4. For  $p = 60\%$ , the PSNR in proposed approach is 11.9% higher compared to MNF, 13.06% higher compared to SBF, 9.76% higher compared to TF and 7.63% higher compared to ADWMF + IAADM model. Similarly, the results for average of FSIM for different values of  $\sigma$  at  $p=50\%$  and at  $p=60\%$  is also tabulated in Table 4. The FSIM obtained by implementing the proposed approach is 2.02% higher compared to MNF, 2.24% higher compared to SBF, 2.6% higher compared to TF and 1.15% higher compared to ADWMF + IAADM model at  $p = 50\%$  distribution of mixed noise. At  $p = 60\%$  distribution of mixed noise, the value of FSIM obtained for SACNN is 13.40% higher compared to MNF, 10.87% higher compared to SBF, 10.66% higher compared to TF and 17.33% higher compared to ADWMF + IAADM model. The PSNR and FSIM value obtained by various filters for  $p=50\%$  and  $p=60\%$  with respect to different values of standard deviation  $\sigma$  is pictorially depicted in Figs. 8 and 9 respectively.

The results for MAE and SSIM for different values of  $\sigma$  at  $p = 50\%$  and at  $p = 60\%$  is given in Table 5. As observed from the Table 5, MAE value is 170% lower compared

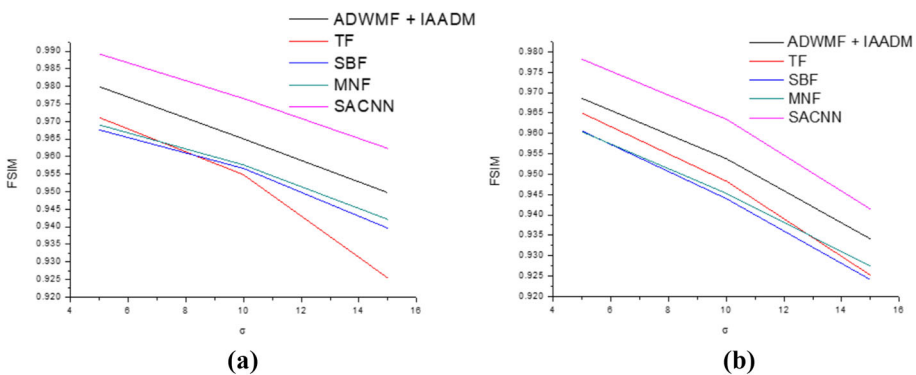


**Fig. 9** (a) Comparison of FSIM at  $p = 50\%$  (b) Comparison of FSIM at  $p = 60\%$

**Table 5** Average MAE and Average SSIM at  $p = 50\%$  and  $p = 60\%$

$\sigma$	Avg. MAE					Avg. SSIM					
	ADWMF	TF	SBF	MNF	SACNN	ADWMF	TF	SBF	MNF	SACNN	
	+					+					
	IAADM					IAADM					
<b>p = 50 %</b>	<b>5</b>	1.18	0.85	0.96	0.99	<b>0.27</b>	0.872	0.901	0.913	0.893	<b>0.994</b>
	<b>10</b>	1.66	1.26	1.46	1.55	<b>0.54</b>	0.822	0.872	0.892	0.852	<b>0.986</b>
	<b>15</b>	2.31	1.67	1.81	1.94	<b>0.85</b>	0.791	0.841	0.854	0.821	<b>0.977</b>
<b>p = 60%</b>	<b>5</b>	1.35	0.89	1.13	1.10	<b>0.38</b>	0.871	0.891	0.901	0.873	<b>0.984</b>
	<b>10</b>	1.71	1.31	1.54	1.62	<b>0.79</b>	0.833	0.873	0.881	0.841	<b>0.971</b>
	<b>15</b>	2.38	1.71	1.86	1.98	<b>0.93</b>	0.782	0.842	0.849	0.811	<b>0.962</b>



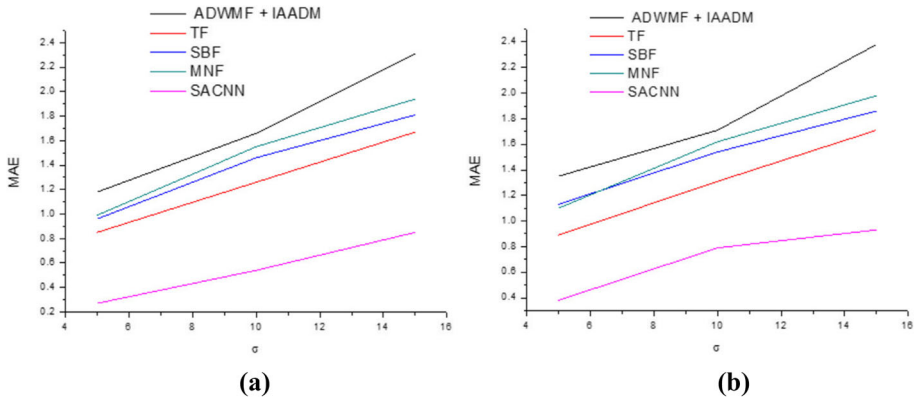


**Fig. 10** (a) Comparison of MAE at  $p = 50\%$  (b) Comparison of MAE at  $p = 60\%$

to MNF, 60% lower compared to SBF, 128% lower compared to TF and 68% lower compared to ADWMF + IAADM model at  $p = 50\%$  distribution of mixed noise. The table also depicts the value of MAE at 60% distribution of mixed noise. For  $p = 60\%$ , the value of MAE is 123% lower compared to MNF, 54% lower compared to SBF, 86% lower compared to TF and 61% lower compared to ADWMF + IAADM model. The results for average of SSIM for different values of  $\sigma$  at  $p=50\%$  and at  $p=60\%$  is listed in Table 5, above. The SSIM in proposed solution is 13.05% higher compared to MNF, 11.20% higher compared to SBF, 11.6% higher compared to TF and 18.99% higher compared to ADWMF + IAADM model at 50% distribution of mixed noise. At  $p=60\%$  distribution of mixed noise, the SSIM is 13.40% higher compared to MNF, 10.87% higher compared to SBF, 10.66% higher compared to TF and 17.33% higher compared to ADWMF + IAADM model. For different values of  $\sigma = 5, 10$  and  $15$ , the values of MAE and SSIM obtained by various approaches are shown in Figs. 10 and 11 respectively.

### 4.3 Discussion

The performance of the proposed SACNN is also investigated by considering different patches having size of  $21 \times 21$ ,  $34 \times 34$  and  $41 \times 41$ . The default patch size in our proposed SACNN filter is  $21 \times 21$ . The simulation results obtained in terms of values of PSNR,

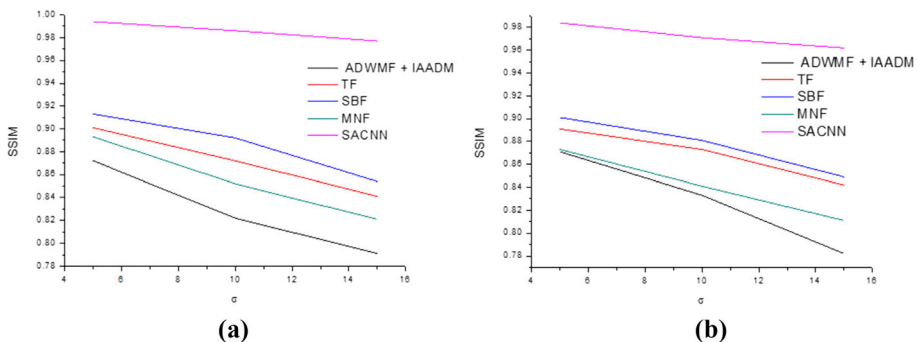


**Fig. 11** (a) Comparison of SSIM at  $p = 50\%$ ; (b) Comparison of SSIM at  $p = 60\%$

**Table 6** Performance for different patch size

Patch size	PSNR	FSIM	MAE	SSIM
21 × 21	33.71	0.9792	0.31	0.965
34 × 34	35.71	0.9892	0.27	0.994
41 × 41	34.42	0.9812	0.38	0.971

FSIM, MAE and SSIM by applying our proposed SACNN filter on US images are noted in Table 6. In order to analyze the performance of our proposed SACNN filter visually, bar graphs are shown in Fig. 12, and we observe that the results are better when we take the patch size of  $34 \times 34$  as compared to any other patch size for any of the four performance matrices. From the simulation results it is observed that the performance of the proposed SACNN filter performance degrades with the increase or decrease of the size of patches.

The RMSE is less while the Crammer and Singer Hinge loss function is considered in our algorithm. The time taken for denoising by all the five models is also measured and noted in Table 7.

The time taken to arrive at the solution by the proposed method is found to be less as compared to existing works due to use of less number of layers in the cognitive neural network, and there is no separate step of categorization of pixel.

#### 4.4 Statistical analysis

In our proposed algorithm, along with the state-of-the-art approaches we have considered various parameters which are randomly initialized. Due to this, the simulation output also slightly changes in each individual run. To have a fair comparison among the approaches, Sign test and the Wilcoxon Signed rank test which are two well acknowledged statistical analysis for pairwise comparison of performance is investigated. These two tests are employed to show the dominance of the proposed SACNN model over others. We have run all the approaches for 25 times each and noted the performance matrices every time. The minimum required numbers for achieving victories significance levels of  $\alpha = 0.05$  and  $\alpha = 0.01$  by running the algorithms for 25 times is shown in Table 8. By considering the PSNR value as victorious parameter, comparison among the algorithms is shown in Table 9. Table 10 depicts that the SACNN has a significant advantage over the other models, with a magnitude of  $\alpha = 0.05$ .

By taking the same PSNR value, the sign test p-value and h-value as the triumphant parameter is depicted in Table 11. The Friedman test between the two algorithms is shown in Tables 12 and 13 which is also used to detect dominance activity.

## 5 Conclusion

The importance of medical images in efficient decision making in terms of diagnosis and prognosis of medical conditions is unprecedented in the current era. There are many ways through which noises gets incorporated in the images that corrupts the quality of the images texture wise as well as at the pixelate level. The most dominant noises are the gaussian and impulse in medical images. During the noise removal, the texture information gets affected, thereby loosing some edge information, which is a major parameter in the process of medical image diagnosis. To address these challenges, the current work proposes a

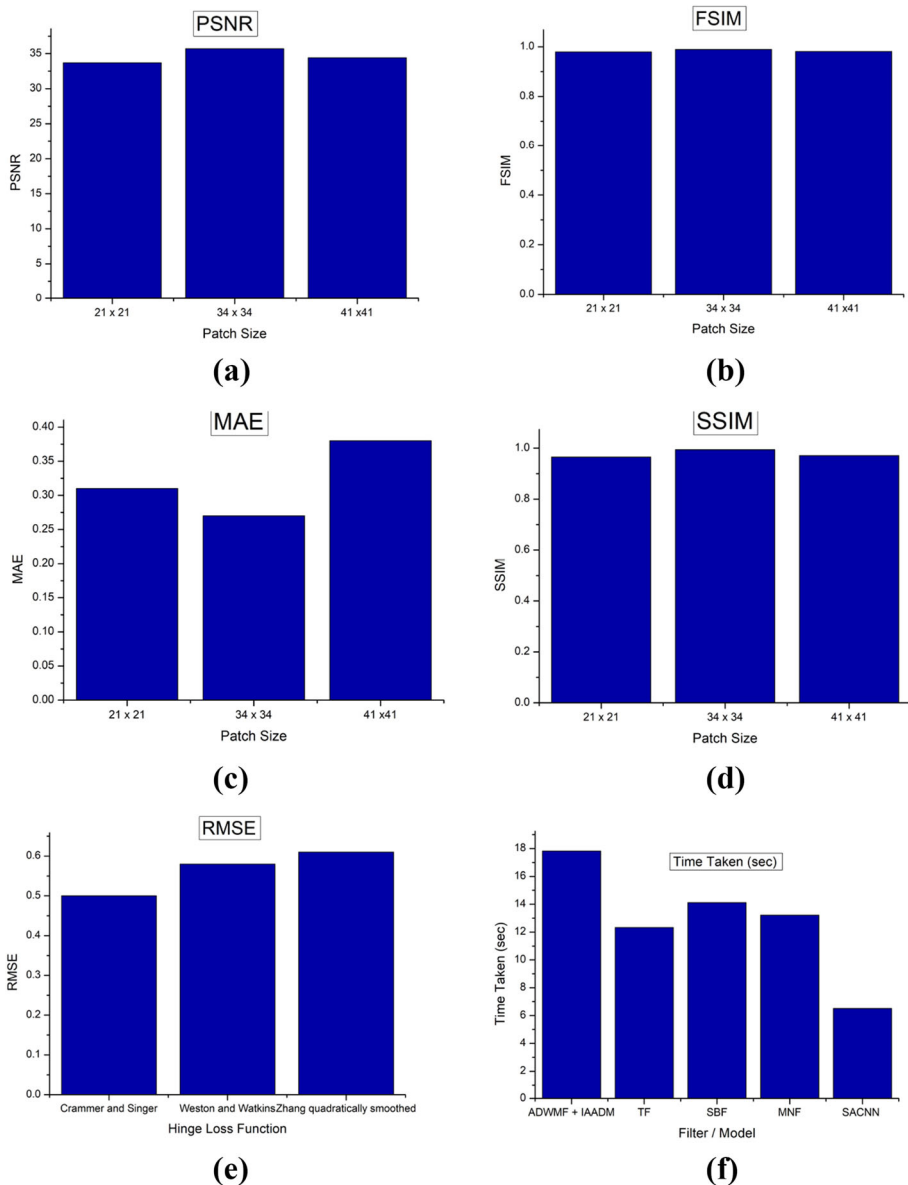


**Fig. 12** Results in terms of Bar graphs (a)PSNR for different patch size (b)FSIM for different patch size (c)MAE for different patch size (d) SSIM for different patch size (e)RMSE across hinge loss functions (f)Comparison of time taken

two-stage cognitive learning assisted model named as SACNN that handles the dual problems of mixed noise removal and edge preservation simultaneously. Mixed noise removal is achieved in the stage1 using the patch transformation and the edges are preserved in the stage 2 through the bilateral filtering. The SACNN model is trained with the noisy as well as noise free image patches. Furthermore, the training data include the edge features of

**Table 7** Comparison of time taken by different methods

Methods	Time taken (sec)
ADWMF + IAADM [23]	17.82
TF [8]	12.32
SBF [20]	14.12
MNF [19]	13.21
<b>SACNN (Proposed)</b>	<b>6.51</b>

**Table 8** Minimum number of wins required to achieve significance levels of  $\alpha = 0.05$  and  $\alpha = 0.01$

No. of cases	7	8	9	10	11	12	13	14	15	16	17	18	19	20	21	22	23	24	25
$\alpha = 0.05$	7	7	8	9	9	10	10	11	12	12	13	13	14	15	15	16	17	18	18
$\alpha = 0.01$	6	7	7	8	9	9	10	10	11	12	12	13	13	14	14	15	16	16	17

**Table 9** Critical value for the two tailed sign tests achieved  $\alpha = 0.05$  and  $\alpha = 0.01$  using loss of energy as victorious parameter

SACNN	MNF	SBF	TF	ADWMF+IAADM
Wins (+)	20	18	17	17
Loss (-)	0	2	3	3
Detected difference	$\alpha = 0.05$	$\alpha = 0.05$	$\alpha = 0.05$	$\alpha = 0.05$

**Table 10** Sign test using PSNR score as a victorious parameter

Comparison	p-value	h-value
SACNN to MNF	0.0009	1
SACNN to SBF	0.0004	1
SACNN to TF	0.0005	1
SACNN to (ADWMF + IAADM)	0.0009	1

**Table 11** Wilcoxon signed test with PSNR score as winning parameter

Comparison	p-value	h-value
SACNN to MNF	0.0009	1
SACNN to SBF	0.0004	1
SACNN to TF	0.0005	1
SACNN to (ADWMF + IAADM)	0.0009	1

**Table 12** Ranking table for the Friedman test

Methods	SBF	MNF	TF	ADWMF + IAADM	SACNN
Mean Ranks	16.8	5.2	8.2	17.2	18

**Table 13** Parameter for the Friedman test

Source	Sum of Square	Degree of Freedom	Mean Square	Chi-Square	Critical value(p)
Column	142.2	3	34.163	55.45	1.782E-11
Error	57.9	75	0.785		
Total	198	100			

the image patches. From the experimental results shows that the proposed approach successfully removed the mixed noise and preserve edges efficiently outperforming some other state-of-the-art filters in term of PSNR, FSIM, MAE and SSIM. The experiments have been conducted with different medical images with  $\sigma = 5, 10, 15$  and  $p = 50\%, p = 60\%$ . The experimental results shows its superiority with an average *PSNR* value in the range of 31.92 to 35.71 and an average *FSIM* value in the range of 0.9414 to 0.9892. From the statistical analysis, it is observed that the proposed two-stage SACNN approach has a significant advantage with a magnitude of  $\alpha = 0.05$  over other four models by considering *PSNR* as victorious parameter. In future, the performance of the proposed solution can be further improved by constructing the multi attributed cost function compared to only Hinge based cost function. Also, the performance of the proposed work may be investigated by considering some other noise. Moreover, some other optimization learning process may be explored for accessing the efficacy of the proposed work. Other modalities of medical images may be considered for investigating the performance of proposed model.

## Declarations

Medical Images for the study in this research have been obtained from Om Hospital, Raipur and patients' identity have not been disclosed. The authors declare that there are no conflicts of interest.

## References

- Al-Sbou YA (2012) Artificial neural networks evaluation as an image denoising tool. *World Appl Sci J* 17(2):218–227
- Brox T, Van Den Boomgaard R, Lauze F, Van De Weijer J, Weickert J, Mrázek P, Kornprobst P (2006) Adaptive structure tensors and their applications. In: *Visualization and processing of tensor fields* (pp 17–47). Springer, Berlin, Heidelberg
- Buades A, Coll B, Morel JM (2005) A non-local algorithm for image denoising. In: *2005 IEEE Computer Society Conference on Computer Vision and Pattern Recognition (CVPR'05) (Vol 2, pp 60–65)*. IEEE
- Chen P, Qian H, Zhu M (2008) Fast Gaussian particle filtering algorithm. 36. 291–294
- Crammer K, Singer Y (2001) On the algorithmic implementation of multiclass kernel-based vector machines. *J Mach Learn Res* 2(Dec):265–292
- Fan L, Zhang F, Fan H, Zhang C (2019) Brief review of image denoising techniques. *Vis Comput Ind Biomed Art* 2(1):1–12
- Fu B, Xiong X, Sun G (2011) An efficient mean filter algorithm. In: *The 2011 IEEE/ICME International conference on complex medical engineering* (pp 466–470). IEEE
- Garnett R, Huegerich T, Chui C, He W (2005) A universal noise removal algorithm with an impulse detector. *IEEE Trans Image Process* 14(11):1747–1754
- Goyal B, Agrawal S, Sohi BS (2018) Noise issues prevailing in various types of medical images. *Biomed Pharmacol J* 11(3):1227
- Goyal B, Dogra A, Agrawal S, Sohi BS (2017) Significance of noise reduction in medical datasets for accurate diagnosis. *Int J Comput Appl* 64(14):1–12

11. Guo F, Zhang C (2019) Edge preserving mixed noise removal. *Multimed Tools Appl* 78(12):16601–16613
12. Hu H, Li B, Liu Q (2016) Removing mixture of gaussian and impulse noise by patch-based weighted means. *J Sci Comput* 67(1):103–129
13. Huang T, Yang GJTG, Tang G (1979) A fast two-dimensional median filtering algorithm. *IEEE Trans Acoust Speech Signal Process* 27(1):13–18
14. Javed SG, Majid A, Mirza AM, Khan A (2016) Multi-denoising based impulse noise removal from images using robust statistical features and genetic programming. *Multimed Tools Appl* 75(10):5887–5916
15. Kumar M, Mishra SK (2018) Jaya based functional link multilayer perceptron adaptive filter for Poisson noise suppression from X-ray images. *Multimed Tools Appl* 77(18):24405–24425
16. Kumar M, Mishra SK (2020) A comprehensive review on nature inspired neural network based adaptive filter for eliminating noise in medical images. *Curr med imaging* 16(4):278–287
17. Li Y, Li C (2020) A mixed model with multi-fidelity terms and nonlocal low rank regularization for natural image noise removal. *Multimed Tools Appl* 79(43):33043–33069
18. Li C, Li Y, Zhao Z, Yu L, Luo Z (2019) A mixed noise removal algorithm based on multi-fidelity modeling with nonsmooth and nonconvex regularization. *Multimed Tools Appl* 78(16):23117–23140
19. Li B, Liu Q, Xu J, Luo X (2011) A new method for removing mixed noises. *Sci China Inf Sci* 54(1):51–59
20. Lin CH, Tsai JS, Chiu CT (2010) Switching bilateral filter with a texture/noise detector for universal noise removal. *IEEE Trans Image Process* 19(9):2307–2320
21. Liu B, Liu J (2018) Non-local mean filtering algorithm based on deep learning. In: *MATEC Web of Conferences* (Vol 232, p 03025). EDP Sciences
22. Liu B, Liu J (2019) Overview of image denoising based on deep learning. In: *Journal of physics: conference series* (Vol 1176, No 2, p 022010). IOP Publishing
23. Ma H, Nie Y (2018) Mixed noise removal algorithm combining adaptive directional weighted mean filter and improved adaptive anisotropic diffusion model. *Mathematical Problems in Engineering*, 2018
24. Mafi M, Izquierdo W, Cabrerizo M, Barreto A, Andrian J, Rische ND, Adjouadi M (2020) Survey on mixed impulse and Gaussian denoising filters. *IET Image Process* 14(16):4027–4038
25. Naga Srinivasu P, Balas VE (2021) Performance measurement of various hybridized kernels for noise normalization and enhancement in high-resolution MR images. In: *Bio-inspired Neurocomputing* (pp 1–24). Springer, Singapore
26. Nair MS, Shankar V (2013) Predictive-based adaptive switching median filter for impulse noise removal using neural network-based noise detector. *SIViP* 7(6):1041–1070
27. O’Shea K, Nash R (2015) An introduction to convolutional neural networks. arXiv:1511.08458
28. Radlak K, Malinski L, Smolka B (2020) Deep learning based switching filter for impulsive noise removal in color images. *Sensors* 20(10):2782
29. Rahman MA, Wang Y (2016) Learning neural networks with ranking-based losses for action retrieval. In: *2016 13th Conference on Computer and Robot Vision (CRV)* (pp 1–7). IEEE
30. Razlighi QR, Kehtarnavaz N (2009) A comparison study of image spatial entropy. In: *Visual communications and image processing 2009* (Vol 7257, p 72571X). International society for optics and photonics
31. Shi Z, Xu Z, Pang K, Cao Q, Luo T (2018) Dissimilar pixel counting based impulse detector for two-phase mixed noise removal. *Multimed Tools Appl* 77(6):6933–6953
32. Singh Chaplot D, MacLellan C, Salakhutdinov R, Koedinger K (2018) Learning Cognitive Models using Neural Networks. arXiv:1806
33. Siva Sai JG, Srinivasu PN, Sindhuri MN, Rohitha K, Deepika S (2021) An Automated segmentation of brain MR image through fuzzy recurrent neural network. In: *Bio-inspired neurocomputing* (pp 163–179). Springer, Singapore
34. Turkmen I (2014) Removing random-valued impulse noise in images using a neural network detector. *Turk J Electr Eng Comput Sci* 22(3):637–649
35. Turkmen I (2016) The ANN based detector to remove random-valued impulse noise in images. *J Vis Commun Image Represent* 34:28–36
36. Wang Y, Scott CD (2020) Weston-Watkins Hinge Loss and Ordered Partitions. arXiv:2006.07346
37. Wang SS, Wu CH (2009) A new impulse detection and filtering method for removal of wide range impulse noises. *Pattern Recogn* 42(9):2194–2202
38. Xiong B, Yin Z (2011) A universal denoising framework with a new impulse detector and nonlocal means. *IEEE Trans Image Process* 21(4):1663–1675
39. Zhang B, Allebach JP (2008) Adaptive bilateral filter for sharpness enhancement and noise removal. *IEEE Trans Image Process* 17(5):664–678

40. Zhang M, Gunturk B (2008) A new image denoising method based on the bilateral filter. In: 2008 IEEE International conference on acoustics, speech and signal processing (pp 929–932). IEEE
41. Zhang L, Zhang X (2003) Global Linear and Quadratic One-step Smoothing Newton Method for P0-LCP. *J Glob Optim* 25(4):363–376
42. Zhang K, Zuo W, Chen Y, Meng D, Zhang L (2017) Beyond a gaussian denoiser: Residual learning of deep CNN for image denoising. *IEEE Trans Image Process* 26(7):3142–3155
43. Zhang K, Zuo W, Gu S, Zhang L (2017) Learning deep CNN denoiser prior for image restoration. In: Proceedings of the IEEE conference on computer vision and pattern recognition, pp 3929–3938

**Publisher's note** Springer Nature remains neutral with regard to jurisdictional claims in published maps and institutional affiliations.

Springer Nature or its licensor (e.g. a society or other partner) holds exclusive rights to this article under a publishing agreement with the author(s) or other rightsholder(s); author self-archiving of the accepted manuscript version of this article is solely governed by the terms of such publishing agreement and applicable law.